Range Image Segmentation Using Surface Selection Criterion

Alireza Bab-Hadiashar, *Senior Member, IEEE,* and Niloofar Gheissari

***Abstract*—In this paper, we address the problem of recovering the true underlying model of a surface while performing the segmentation. First, and in order to solve the model selection problem, we introduce a novel criterion, which is based on minimising strain energy of fitted surfaces. We then evaluate its performance and compare it with many other existing model selection techniques. Using this criterion, we then present a robust range data segmentation algorithm capable of segmenting complex objects with planar and curved surfaces. The presented algorithm simultaneously identifies the type (order and geometric shape) of each surface and separates all the points that are part of that surface. This paper includes the segmentation results of a large collection of range images obtained from objects with planar and curved surfaces. The resulting segmentation algorithm successfully segments various possible types of curved objects. More importantly, the new technique is capable of detecting the association between separated parts of a surface, which has the same Cartesian equation while segmenting a scene. This aspect is very useful in some industrial applications of range data analysis.**

***Index Terms*—Model selection, range data, robust range data segmentation, scale estimation.**

I. Introduction

MANY computer vision algorithms rely on using a parametric model, which is usually determined by examining the underlying physical phenomenon. Such physical constraints are often represented by a family of parametric models that can be applicable to a task performed in various situations [3], [18], [26], [41]–[44]. Hence, a complete solution to most vision tasks is likely to depend on how well the true underlying model is chosen.

On the other hand, the model selection problem, which refers to choosing the most appropriate and concise model to express given data in an abstract fashion, has been studied by statisticians for many decades. Since the introduction of Akaike's Information Criterion (AIC) [1], which had a fundamental effect on model selection research, many model selection criteria have been introduced (i.e., [9] and [25]) and many of those model selection techniques have been employed in many computer vision algorithms for various applications (i.e., [8] and [10]).

A range image contains three-dimensional (3-D) information about a scene including the depth of each pixel. Segmenting a range image is the task of dividing the image into regions so that all the points of the same surface belong to the same region, there is no overlap between different regions and the union of these regions generate the entire image.

There have been two main approaches to the range segmentation problem: region-based and edge-based approaches. Region-based range segmentation algorithms can be categorised into two major groups: parametric model-based range segmentation algorithms and region-growing algorithms.

Algorithms of the first group, such as the algorithm proposed here, are based on assuming a parametric surface model and grouping data points so that all of them can be considered as points of a surface from the assumed parametric model (an instance of that model). While region-growing algorithms start by segmenting an image into initial regions. These regions are then merged or extended by employing a region growing strategy [14], [33]. These initial regions can be obtained using different methods including iterative or random methods. A drawback of algorithms of this group is that in general they produce distorted boundaries because the segmentation usually is carried out at region level instead of pixel level.

Edge-based range segmentation algorithms are based on edge detection and labelling edges using the jump boundaries (discontinuities). They apply an edge detector to extract edges from a range image. Once boundaries are extracted, edges with common properties are clustered together. A typical example of edge-based range segmentation algorithms is presented by Fan *et al.* [13]. The segmentation procedure starts by detecting discontinuities using zero-crossing and curvature values. The image is segmented at discontinuities to obtain an initial segmentation. At the next step, the initial segmentation is refined by fitting quadratics whose coefficients are calculated based on the least squares method.

In general, a drawback of edge-based range segmentation algorithms is that although they produce clean and well-defined boundaries between different regions, they tend to produce gaps between boundaries. In addition, for curved surfaces, discontinuities are smooth and hard to locate, and, therefore, these algorithms tend to under-segment the range image.

Although the range image segmentation problem has been studied for a number of years, the task of segmenting range images of curved surfaces is yet to be satisfactorily resolved. The comparative survey of Powell *et al.* [34] reveals the challenges that need to be addressed.

Manuscript received May 8, 2004; revised September 7, 2005. N. Gheissari was supported by Swinburne University of Technology under a postgraduate scholarship. The associate editor coordinating the review of this manuscript and approving it for publication was Dr. Eli Saber.

A. Bab-Hadiashar is with the Faculty of Engineering and Industrial Sciences, Swinburne University of Technology, Melbourne, Australia (e-mail: abab-hadiashar@swin.edu.au).

N. Gheissari was with the Faculty of Engineering and Industrial Sciences, Swinburne University of Technology, Melbourne, Australia. She is now with National ICT Australia, Australian National University, Canberra, Australia (e-mail: niloofar.gheissari@nicta.com.au).

Digital Object Identifier 10.1109/TIP.2006.877064

A. Range Segmentation of Curved Surfaces

There have been various studies of fitting higher order surfaces to, and also range segmentation of, curved surfaces. Most of those techniques are limited due to the fact that they have assumed the underlying model for every surface is an *a priori* known proposition. For example, Marshall *et al.* [32] presented a linear method for fitting cylindrical, conical, spherical and tori surfaces (for each surface separately).

Werghi *et al.* [49] presented a method for surface fitting which has the advantage of considering maximum information in the scene including the relationship between different surfaces. Although this approach appears to be reliable for reverse engineering purposes, this method has a drawback. That is, the correct underlying model for each surface in the scene is assumed to be known. Therefore, such approaches are not suitable for computerised range segmentation applications. Gaussian and Mean Curvature signs also have been widely used in identifying surface types in various range segmentation schemes [5], [12]. The biggest drawback of this method is that the signs of Gaussian and Mean Curvatures are very sensitive to noise and quantisation error. Thus, usually one needs to set some heuristic thresholds that have little theoretical justifications. Another disadvantage of using curvature signs is that the higher order surfaces are only limited to the eight different possible cases that are determined by Gaussian and Mean curvature signs. Therefore, this method is not applicable to identify more realistic surfaces like conical, spherical, etc.

Using a model selection criterion for detecting the correct underlying surface for range segmentation application was pioneered by Boyer *et al.* [8]. They presented a robust range segmentation algorithm capable of segmenting higher order surfaces using a Modified CAIC as a surface model selection criterion. This technique has only been tested on synthetic range data with limited success. It appears that except for the above work, there has not been any other work on choosing the underlying model from a library of models prior to segmenting the data.

B. Evaluating Range Segmentation Algorithms

Evaluation of the quality of range segmentation techniques has also received some attention during the last decade. An early work, which aimed at evaluating range segmentation algorithms, was published by Trucco and Fisher [47]. They investigated the effect of changing algorithms' input parameters (thresholds, etc.) on the estimated curvature of the segmented regions.

Hoover *et al.* [21] were perhaps the first to present a comprehensive method for evaluating range segmentation algorithms. They classified different possible results of a range segmentation algorithm into: correct detection, over segmentation, under segmentation, missed classification and noise classification. Then, they evaluated some well-known range segmentation algorithms including USF [17], WSU [19], UB [23], and UE [15] using this classification. They concluded that among the evaluated algorithms, UE has a higher percentage of success in detecting the correct segments. Another attempt in this direction was reported by Jiang *et al.* [22] in which they evaluated three more range segmentation algorithms including OU [22], PPU [6], [7], and UA. [30].

Although the work of Hoover *et al.* was limited to evaluating segmentation algorithms of planar surfaces only, their evaluating method can be easily extended to curved objects segmentation. Using their method Powell *et al.* [34] evaluated the performance of two range segmentation algorithms (UB [23] and BJ [5]) capable of segmenting curved objects. As they reported, the results indicated that the range segmentation of curved objects is much more involved and none of the existing techniques appears to be satisfactory. Although they recommended the UB over BJ technique due to its higher average of correct detections, they concluded that UB tends to highly under-segment an image.

In this paper, we propose a new approach to the model selection problem based on physical constraints rather than statistical characteristics. Our approach is motivated by our observations that none of the existing model selection criteria is capable of recovering the underlying model of range data of curved objects [4]. In addition and in order to demonstrate the effectiveness of our proposed model selection criterion, we have devised and fully tested a robust model-based range segmentation algorithm for curved objects (not limited to planar surfaces). Our range segmentation algorithm is capable of detecting the association between separated parts of a surface, all of which has the same Cartesian equation.

To choose the appropriate surface model from a library of models, we propose a new model selection technique called Surface Selection Criterion (SSC), which is based on the minimisation of the bending and twisting energy of a thin surface. The proposed model selection techniques and its implementation for range segmentation are explained in detail in Sections II and III. Recovering the underlying model is a crucial aspect of segmentation when the objects are not limited to having planar surfaces only (so more than one possible candidate model exists). An important aspect of having a correct model is that it makes it possible to recover the true surface parameters while segmenting the data.

For comparison, we first use the method of Hoover *et al.* to evaluate the performance of our segmentation algorithm on the ABW range database. This allows us to compare and benchmark the performance of our technique on planar objects with the previously published results ([21], [29], and [34]) before we proceed to the main task of segmenting curved objects.

For evaluating the performance and benchmarking the proposed technique for segmenting curved objects, we have gathered a large collection of range images containing both planar and quadratic surfaces (our range image database will be made publicity available upon the acceptance of this paper). For benchmarking, however, we have applied the method of Hoover *et al.* to evaluate our algorithm (using the above database) and compare with UB [28] technique (as the most promising technique). The results of our experiments are presented in Section IV. Section V concludes the paper.

II. Model Selection

The main contribution of this paper is the introduction of a new model selection technique to identify the appropriate model from a family of models representing possible surfaces of curved objects. During the last three decades, due to its

TABLE I
DIFFERENT MODEL SELECTION CRITERIA STUDIED IN THIS PAPER

Name	Criterion	Introduced by
AIC	$\sum_{i=1}^{N} r_i^2 + 2P\delta^2$	Akaike [1]
MDL	$\sum_{i=1}^{N} r_i^2 + (P/2)\log(N)\delta^2$	Rissanen [35]
GBIC	$\sum_{i=1}^{N} r_i^2 + (Nd\ \log(4) + P\ \log(4N))$	Heckerman and Chickering [11]
G-CP	$\sum_{i=1}^{n} r_i^2 + (2(dN + P) - mN)\delta^2$	Kanatani [28]
CP	$\sum_{i=1}^{n} r_i^2 + (-N + 2P)\delta$	Mallow [31]
GAIC	$\sum_{i=1}^{N} r_i^2 + 2(dN + P)\delta^2$	Kanatani [27]
GIC	$GIC = \sum_{i=1}^{N} r_i^2 + \lambda_1 dN\delta^2 + \lambda_2 P\delta^2$	Torr [45,46]
SSD	$\sum_{i=1}^{N} r_i^2 + (P\log(N+2)/24 + 2\log($	Rissanen [36]
CAIC	$\sum_{i=1}^{N} r_i^2 + P(\log N + 1)\delta^2$	Bozdogan [9]
CAICF	$\sum_{i=1}^{N} r_i^2 + P(\log N + 2)\delta^2 + \log\lvert J$	Bozdogan [9]
BMSC-BAYES	$P/2 \log 2\pi - \sum_{i=1}^{N} r_i^2 / \delta^{*2}{}_{m\,high} + 1/$	Bubna and Stewart [10]
BAYES	$(2\pi)^{P/2} L(\hat{\theta}_m)\sqrt{1/\sum_{i=1}^{N} r_i^2}$	Schwart [39]
MCAIC	$(1+f)\sum_{i=1}^{N} W_i \log\left[1 + \frac{r_i^2}{f\theta^2}\right]$	Boyer et al.[8]
GMDL	$\sum_{i=1}^{N} r_i^2 - (Nd + P)\varepsilon^2 \log(\delta / L)^2$	Kanatani [27]

various applications in statistics, engineering and science, many model selection criteria [1], [9], [27], [37], [42] have been proposed which almost all have their roots in statistical analysis of the measured data. The proposed Surface Selection Criterion (SSC) is based on the minimizing of the strain energy of a thin plate rather than statistical assumptions.

To illustrate the efficiency of the proposed criterion, we evaluate and compare the SSC with some existing (presented previously in the literature) model selection criteria. A brief overview of the considered model selection criteria is shown in Table I. In this table, Σr_i^2 is the sum of squared residuals and δ is the scale of noise. N is the number of points, P is the number of parameters and d is the dimension of the surfaces (here 2). J is the fisher matrix of the estimated parameters. L, the reference length, is set to be N, m is the dimension of the data (here 3) and $\hat{\theta}_m$ is the estimated parameters of each model. f is the number

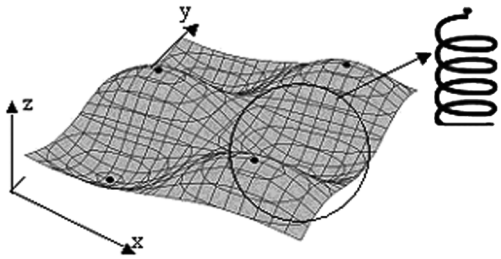

Fig. 1. Representation of a malleable surface supported by hypothetical springs. The range measurements are shown by black circles.

of degrees of freedom of the assumed t distribution for MCAIC (here 1.5). Finally, Wi is the associated weight for each point in MCAIC (see [8] for more details) and $V*$ is the covariance matrix of parameters [10].

A. Surface Selection Criterion

Our proposed criterion is based on minimising the sum of bending and twisting energy of all possible surfaces in a model library. Although the bending energy of a surface has been used in the literature for motion tracking and finding parameters of deformable objects [48], it appears that the bending energy of a surface has not been previously used for model selection purposes. An approximation to the energy of a surface has also been utilised in spline fitting using a thin plate analogy. We, too, follow this type of analogy.

To formulate our model selection criterion, we view the range data of different points of an object as hypothetical springs constraining the surface as shown in Fig. 1. If the surface has little stiffness, then the surface passes close to measurements (fits itself to the noise) and the sum of squared residuals between the range measurements and their associated points on the surface will be small (the sum of squared residuals in this analogy, relates to the energy of the deformed springs).

However, to attain such proximity, the surface has to bend and twist in order to be close to the measured data. This in turn increases the amount of strain energy accumulated by the surface.

For model selection, we propose to view the sum of bending and twisting energies of the surface as a measure of surface roughness and the sum of squared residuals as a measure of fidelity to the true data. A good model selection criterion should, therefore, represent an acceptable compromise between these two factors. As one may expect, increasing the number of parameters of a surface leads to a larger bending and twisting energies as the surface has more degrees of freedom and consequently the surface can be fitted to the data by bending and twisting itself so that a closer fit to measured data results [this can be inferred from the bending energy formula (1)]. However, the higher the number of parameters for a surface model assumed, the less the sum of squared residuals is going to be. For instance, in the extreme case, if the number of parameters is equal to the number of data points (which are used in the fitting process), then the sum of squared residuals will be zero whereas its sum of energies will be maximised.

As shown in [40], if a plate is bent by a uniformly distributed bending moment so that the xy and yz planes are the prin-

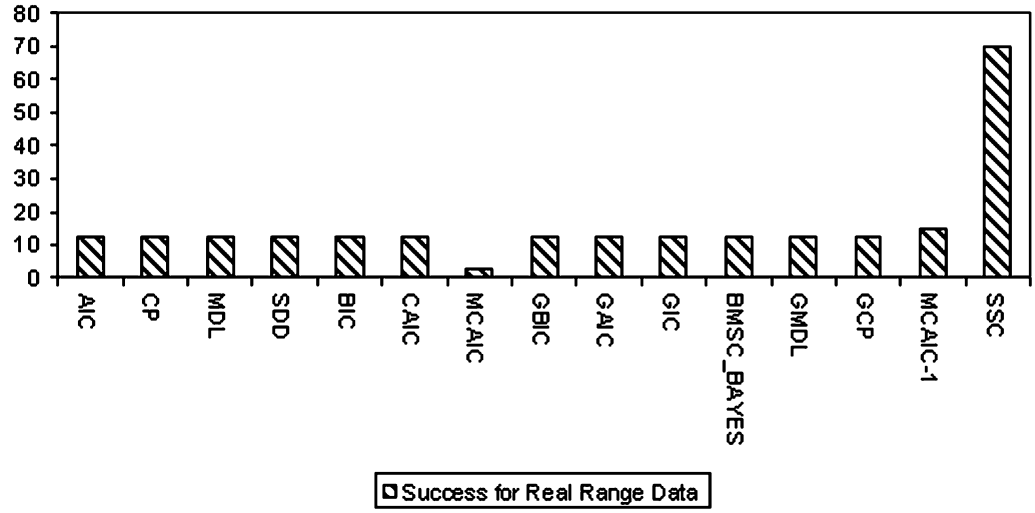

Fig. 2. Success rate (percentage of success) of various model selection criteria on real range data.

cipal planes of the deflected surface, then the strain energy (for bending and twisting) of the plate can be expressed as

$$E_{\text{Bending+Twist}} = \int\int \frac{1}{2}D\left\{\left(\frac{\partial^2 w}{\partial x^2}+\frac{\partial^2 w}{\partial y^2}\right)^2 -2(1-\nu)\left[\frac{\partial^2 w}{\partial x^2}\frac{\partial^2 w}{\partial y^2}-\left(\frac{\partial^2 w}{\partial x \partial y}\right)^2\right]\right\} dxdy \quad (1)$$

where D is the flexural rigidity of the surface and ν is Poisson's ratio (ν should be very small because in real world-objects the twisting energy in comparison with the bending energy is small). In our experiments we assume $\nu = 0.01$. We found in our experiments that the performance of SSC is not overly sensitive to the small variation of this value. In order to scale the strain energy, we divide its value by the strain energy of the model with the highest number of parameters ($E_{\max}$). Therefore, D will be eliminated from our computation.

To capture the trade-off between the sum of squared residuals $\sum_{i=1}^{N} r_i^2$ and the strain energy $E_{\text{Bending+Twist}}$, we define a function *SSC* such that

$$SSC = \sum_{i=1}^{N}\frac{r_i^2}{N\delta^2} + P\frac{E_{\text{Bending+Twist}}}{E_{\max}}$$

where δ is the scale of noise for the highest surface (the surface with the highest number of parameters). The reason that we use the scale of noise for the highest surface (as explained by Kanatani [28]) is that the scale of noise for the correct model and the scale of noise of the higher order models (higher than the correct model) must be close for the fitting to be meaningful. Therefore, it is the best estimation of the true scale of noise that is available at this stage.

An accurate estimate of the scale of noise δ can be computed by $\delta^2 = \sum_{i=1}^{N} r_i^2/(N-P)$ where N is the number of data points and P is the number of parameters of the highest surface (6 for our model library). Use of this formula for the scale of noise can be justified by the fact that if the model that we assume is correct, then $\sum_{i=1}^{n} r_i^2/\delta^2$ is subjected to a χ^2 distribution with $N-P$ degrees of freedom [28]. The energy term has been multiplied by the number of parameters P in order to discourage choosing a higher order (than necessary) model. Such a simple measure produces good discrimination and improves the accuracy of the model selection criterion.

Having devised a reasonable compromise between fidelity to data and the complexity of the model, our model selection task is then reduced to choosing the surface that has the minimum value of *SSC*.

B. Evaluating and Comparing SSC With Other Model Selection Criterion

To evaluate our proposed Surface Selection Criterion and compare it with other well known model selection criteria (summarised in Table I), we implemented all of the criteria by simply calculating the values in Table I in the same program. Therefore, the residuals applicable to all of criteria were the same and were calculated as the algebraic distance between the predicted point and observed point on the surface. We used the same scale of noise for all the criteria according to $\delta^2 = \sum_{i=1}^{N} r_i^2/(N-P)$ where N is the number of data points (size of the surface in terms of pixels) and P is the number of parameters of the highest model in the library (here 6). All the investigated criteria choose the most appropriate model from the given library by minimising their corresponding mathematical expressions (shown in Table I). To examine the success rate of the SSC and compare it with other selection techniques on real range images, we randomly hand picked points of 50 different real quadratic and planar surfaces and applied different model selection criteria to them. As can be seen from Fig. 2, the proposed criterion (SSC) is considerably better in choosing the right model when it is applied to a variety of real range data.

To fully evaluate *MCAIC*, we have considered two distinct cases based on the values chosen for $W_i s$. In the first set of experiments, W_i is calculated using the formula proposed by Boyer *et al.* [8] as $W_i = ((1+f)/f + (r_i/s)^2)$. We then examined the performance of MCAIC where the effect of these weights (W_i) is removed by setting all to one. The latter is shown by MCAIC-1 in our figures.

TABLE II
LIBRARY OF MODELS USED FROM THE MOST GENERAL TO THE SIMPLEST MODEL USED IN OUR EXPERIMENTS

Model 1	Partial Quadratic Surface	$ax^2+by^2+cz^2+dx+ey+fz=1$
Model 2	5th order conic for example cylinder in z direction	$ax^2+by^2+cx+dy+eyx=1$
Model 3	5th order conic for example cylinder in y direction	$ax^2+bz^2+cx+dz+exz=1$
Model 4	5th order conic for example cylinder in x direction	$az^2+by^2+cz+dy+fyz=1$
Model 5	4th order conic for example cylinder in z direction	$ax^2+by^2+cx+dy=1$
Model 6	4th order conic for example cylinder in y direction	$ax^2+bz^2+cx+dz=1$
Model 7	4th order conic for example cylinder in x direction	$ay^2+bz^2+cy+dz=1$
Model 8	Plane	$ax+by+cz=1$

We have a conjecture as to why using the SSC should be advantageous. As previously described, to choose the correct model, one needs to establish a trade off between "fidelity" (how well a model fits the data, which is often measured by the sum of squared residuals) and the "complexity" of that model. In all the model selection criteria that have been introduced so far, the number of parameters of a model is the only measure of complexity of that model. Thus, the existing model selection criteria work well, only if the candidate models in the model library are nested. It means that there are not models which have the same number of parameters (complexity). In fact, if one applies the existing model selection criteria to some models having the same number of parameters, the choice of "the most appropriate model" will only be based on the goodness of the fit (residuals). The model library shown in Table II includes some example of such models.

The reason that most of the model selection criteria perform the same is that as previously described where there are modes of the same number of parameters; many of the model selection criteria have similar penalty terms. Hence, the selection is only based on the sum of squared residuals, which is identical for almost all criteria.

III. SEGMENTATION ALGORITHM

Having described our method for recovering the underlying model of a higher order surface, we then proceed to use our method to perform the range segmentation of curved objects.

A. Model-Based Range Segmentation Algorithm

The details of the proposed range segmentation algorithm are described below. The proposed algorithm incorporates some elements which have been introduced by Bab-Hadiashar and Suter [2]. In particular, it relies on the Modified Selective Statistical Estimator (MSSE) by which the scale of noise is estimated. The main difference of this algorithm with the algorithm of Bab-Hadiashar and Suter is that it expands a homogenous region iteratively and applies a model selection criterion to this region. It, therefore, enables the new algorithm to segment range images of objects having various types of surfaces including planar, cylindrical, spherical, etc. The new proposed algorithm employs a threshold K, which corresponds to the size of the smallest region that can be regarded as a separate region. This means those structures which contain less than K percent of the whole data are ignored. The other threshold required for this algorithm is T, which corresponds to the desired significance level and can be looked up from the normal distribution table. For example, if 99% significance level is required, T is set to be 2.5.

B. Preprocessing Step

Before applying the segmentation algorithm, pixels whose associated depths are not valid need to be eliminated. The invalid points could appear because of the limitation of the range finder used for measuring the depth (mainly due specularities, poor texture, etc.). The range scanner usually marks these points with an out-of-range number. If there are no such points, this stage is skipped. Then, a random sampling (RANSAC type) method is applied to find an initial homogenous local region, which will be used to recover the true underlying surface model. Detail of the sampling method is described in the next section.

After eliminating invalid pixels, the following tasks are iteratively performed until the number of remaining data points becomes less than K percent of the total number of data points.

Finding an Initial Estimate of the Surface Parameters.

To obtain an initial estimate of the surface parameters, a localised homogenous region inside the data space in which all the pixels lie on a flat plane needs to be found. Even if the current surface is not planar, a very small local area (for example, a square of size 15×15) can be regarded as a planar surface. Since this region is likely to contain some outliers, if a higher order model (than the planar model) is used, some outliers might be classified as inliers.

To find such a region, p random points, which all belong to the same square of size 15×15 -located in an arbitrary place, for local sampling purpose are chosen where p is larger than 3 (number of parameters of a plane). Then, an over-determined system of equations is created according to the 3-D plane equation, i.e., $ax + by + cz = 1$.

In fact, each random point generates a constraint in this equation system. Then, the system of linear equations is solved (using the least square method) and the residuals are calculated according to $r^2 = (ax + by + cz - 1)^2$.

The above steps are repeated a number of times (here, 30 times) and a solution that generates the least median of squared residuals [38] is chosen. Then, the outliers are rejected based on a preliminary estimate of the scale of noise. At this stage, we only need a very conservative estimate of the scale and the following robust estimate is used not since it would provide the best estimate, but because it is a computationally cheap and relatively robust estimate of the noise. One can also use the MSSE at this stage, but that would unnecessarily increase the computation burden. This preliminary estimate is computed according to [38]: $s^0 = 1.4826(1 + (5/P - 2))\sqrt{\text{med}_i r_i^2}$ where P is the number of data points inside the square and r_i corresponds

to the algebraic residual of ith point. Now, every constraint in the equations system (which corresponds to a separate sample point) is to be classified. To achieve this, every constraint whose residual (r_i) is such that $|r_i/s^\circ|$ is greater than a threshold (T) is weighted by zero. It means that the corresponding random point is assumed to be an outlier. Otherwise, the weight is set to 1.

C. Finding a Number of Acceptable Region

If the number of inliers (resulting from the previous step) is more than half the size of the square, this square is marked as an acceptable region. The size of the square used is not critical; however, it needs to be large enough to contain adequate sample points and also to contain more than K percent of the image points that is size of the smallest possible separate region. The square size is set to 15×15 pixels in our experiments.

When an acceptable region is found, the corresponding parameters of the region are fitted to the image points (which are not yet classified) and the residual for each point is calculated.

The above two steps (0 and C) are repeated a number of times so that a number of regions, which are marked as accepted, have been found. Each region corresponds to an acceptable fit. The more these two steps are repeated, the more accurate the results are likely to be. Around 1000 iterations are used in our experiments.

D. Choosing the Most Reliable Data Group Based on the Kth Order Residual

Up to this point, a number of regions (or fits) that are marked as accepted have been found. Among them, the most reliable one is chosen using the modified selective statistical estimator (MSSE) [2]. It means that the fit that generates the least Kth order residual is chosen as the most reliable one. The choice of K depends on the application [2] and is set to 10% in our experiments. This algorithm is not overly sensitive to the value of K. However, if K is set to a very large number, small structures will be ignored.

E. Expanding the Region

As described in [16], the performance of all the model selection criteria is greatly affected by the size of data. If the acceptable region (found in the previous section) is smaller than the minimum required size (for optimal performance of the criterion), to increase the degree of confidence, the chosen localised region can be extended. To achieve this, the following three steps are performed iteratively a few times until the region is large enough so that the model selection criterion can be reliably applied.

The scale of noise is calculated according to the formula

$$\delta^2 = \sum_{i=1}^{N} \frac{r_i^2}{(N-P)}$$

where N is the number of data points and P is the number of parameters of the highest model.

Points whose residual is greater than the scale of noise multiple of T are rejected as outliers and a region of inliers is created.

The surface parameters are then refined by fitting the highest model in the model library.

It should be noted that since the underlying true surface model is yet to be detected, in this step the underlying surface model is assumed to be the most general model. This is because to apply a model selection criterion the scale of noise for the highest model is the most accurate scale of noise available at this stage. In fact, (as explained by Kanatani [28]) the scale of noise for the correct model and the scale of noise of the higher order models (higher than the correct model) must be close for the fitting to be meaningful. In addition, since the outliers are rejected in the previous step, it is safe to use a higher order model.

F. Selecting the Appropriate Surface Model

Having found this local region, any model selection criterion can be applied to identify the true underlying surface model. However, as previously described SSC has shown to be superior in correctly detecting the true model.

To apply the chosen model selection criterion (here SSC) to the extended region, all models in the model library (shown in Table II) are fitted to the extended region and then the values of the criterion for all models are compared and the model that minimises this value is chosen as the appropriate model.

G. Removing Outliers

Before establishing a new segment, all the remaining outliers should be rejected by performing the following tasks.

1) Fitting the Chosen Model to the Data: The chosen model is now fitted to whole data (not segmented parts) and the residuals are computed. Then, the scale of noise is estimated using the technique explained below. The points whose absolute residuals is larger than T multiple of the scale of noise are rejected as outliers. As a result a new coherent segment (containing inliers) is generated.

It is important to note that performing the above step has the advantage of merging the occluded parts of a surface (if there are any). This is due to the fact that every point of this new segment is picked up regardless of its geometrical location. Finally, the points, which are grouped at this stage, are marked as segmented so that they do not participate in the next iterations of the segmentation process.

2) Estimating the Scale of Noise: To estimate the scale of noise for every segment, we use the method presented by Bab-Hadiashar and Suter [2]. This method is based on the idea that when the squared residuals are sorted (and after finding the right model for a segment of any given image) a large jump in the values of sorted residuals will be observed due to the existence of outliers or data of other segments. Location of this jump helps to simultaneously estimate the scale of noise and find the data members of each segment.

H. Hole Filling

Because of invalid and noisy points (where the range finder has not been able to correctly measure the depth mainly due to the surface texture or specularity), there will be some holes in the segmented image. Applying a hole-filling algorithm (here, a

TABLE III
AVERAGE RESULTS OF DIFFERENT SEGMENTATION SCHEMES AND OUR PROPOSED ALGORITHM (80% TOLERANCE—SEE [21] AND [34] FOR DETAILS) FOR 100 SURFACES OF THE ABW DATABASE

Technique	GT regions	Correct Detection	Angle diff. (std dev.)	Over Segmentation	Under Segmentation	Missed	Noise
OU	15.2	9.8	Not Available	0.2	0.4	4.4	3.2
PPU	15.2	6.8	Not Available	0.1	2.1	3.4	2.0
UA	15.2	4.9	Not Available	0.3	2.2	3.6	3.2
USF[17]	15.2	12.7	1.6° (0.8)	0.2	0.1	2.1	1.2
WSU[19]	15.2	9.7	1.6° (0.7)	0.5	0.2	4.5	2.2
UB[23]	15.2	12.8	1.3° (0.8)	0.5	0.1	1.7	2.1
UE[15,47]	15.2	13.4	1.6° (0.9)	0.4	0.2	1.1	0.8
Ubham [29]	15.2	13.4	1.6° (0.8)	0.4	0.3	0.8	1.1
EG[24]	15.2	13.5	Not Available	0.2	0.0	1.5	0.8
Proposed algorithm	15.2	12.81	1.4° (0.9)	0.04	1.55	0.8	Nominal

median filter of 10×10 pixels) to all inliers and removing those holes can improve the appearance of segmentation results.

This stage is only for the sake of the appearance of the results and has no effect on the segmented surface's parameters because the fitting has already been performed. However, some of the missed invalid and noisy points can be grouped in this step. This hole filling stage is purely cosmetic and can be skipped if it is not needed.

IV. EXPERIMENTAL RESULTS

To evaluate the performance of the proposed algorithm, we have conducted an extensive set of experiments using real range images of various objects. The first set of experiments is solely for comparison purposes and is performed on the existing ABW range image database that only includes objects with planar surfaces. It is shown in Section 5.1 that the proposed technique can accurately segment the above database and its performance is similar to the best techniques presented in the literature [21].

We, however, go further and show that our algorithm not only can segment planar surfaces as well as the most efficient algorithms presented in the literature, but also that it is capable of reliably segmenting parametric curved objects. To do so, we have applied our technique to a set of real range images with objects having a combination of planar and curved surfaces. In Sections IV-B and IV-C, it is shown that the present technique is capable of correctly segmenting those objects and identifying the underlying model of each surface, simultaneously.

A. ABW Image Database

In the first set of our experiments, we tested the proposed algorithm on the ABW [20] range image database and compared our results with the ones reported in the literature. As it is shown in the following figures, the proposed technique is able to segment all of the images correctly. A summary of segmentation results (statistical measures) for the entire ABW database (30 images) is shown and compared with other techniques in Table III.

Moreover, We measured the performance of our algorithm in estimating angles and comparing it with the results obtained by Hoover *et al.* [21]. To achieve this, we calculated the absolute difference between the real angle (calculated using the IDEAS CAD package) and the computed angle using the parameters of the segmented surface. However, since computing the real angle using the IDEAS CAD package was a time consuming task, we randomly hand picked up 100 surfaces and the angle difference was calculated only for those surfaces. The average and the standard deviation of the error for our technique and others reported in the literature are shown in Table III. Some segmented samples on the ABW images are shown in Fig. 3. This figure shows that the propose algorithm has generated clean and accurate segmentation results.

B. K2T Database

As we mentioned before, the proposed algorithm is based on using parametric models to describe curved surfaces. The K2T range image database is the only existing database that has been used in literature to evaluate two range segmentation algorithms in segmenting curved objects (by Powel *et al.* [34]).

To demonstrate that the proposed technique can successfully segment objects of the K2T database (ones with parametric surfaces), an example containing a curved object (a donut shape object represented by a torus surface) is chosen and the proposed algorithm is applied to segment the object from its backgrounds. The following Figs. 4 and 5 show the result of segmentation and its comparison with UB algorithm. The rational behind selecting UB as a benchmark is that according to [21] and [34], UB has the most promising performance amongst other evaluated range segmentation algorithms capable of segmenting curved surfaces.

As can be seen from these figures, while the UB algorithm generates a large number of noisy and misclassified points, the proposed algorithm has generated good segmentation with clean regions. It is also important to note that the proposed.

Surface selection criterion (SSC) has been successful in recovering the true underlying models for both planar and curved surfaces.

C. Curved Objects Database

To evaluate the performance of our algorithm in segmenting range images of curved objects, we created a range image database of a number of objects possessing both planar and curved surfaces from different materials. The actual data and their segmented results are shown in the following figures (Figs. 6–15). The statistics of the results, based on the method of Hoover et al., are also shown in Table IV.

To compare and benchmark the performance of our algorithm with other well-known range segmentation algorithms we have applied the publicly available implementation of the UB algorithm to our range database. For the sake of comparison, we have generated their results in terms of the same metrics used by Hoover *et al.* The results of this comparison are shown in Table IV which demonstrates that the proposed algorithm performs considerably better than UB.

Due to the fact that for the 3 images shown in Figs. 6–8 we only have the (x, y, z) data and not the full set (range data of a

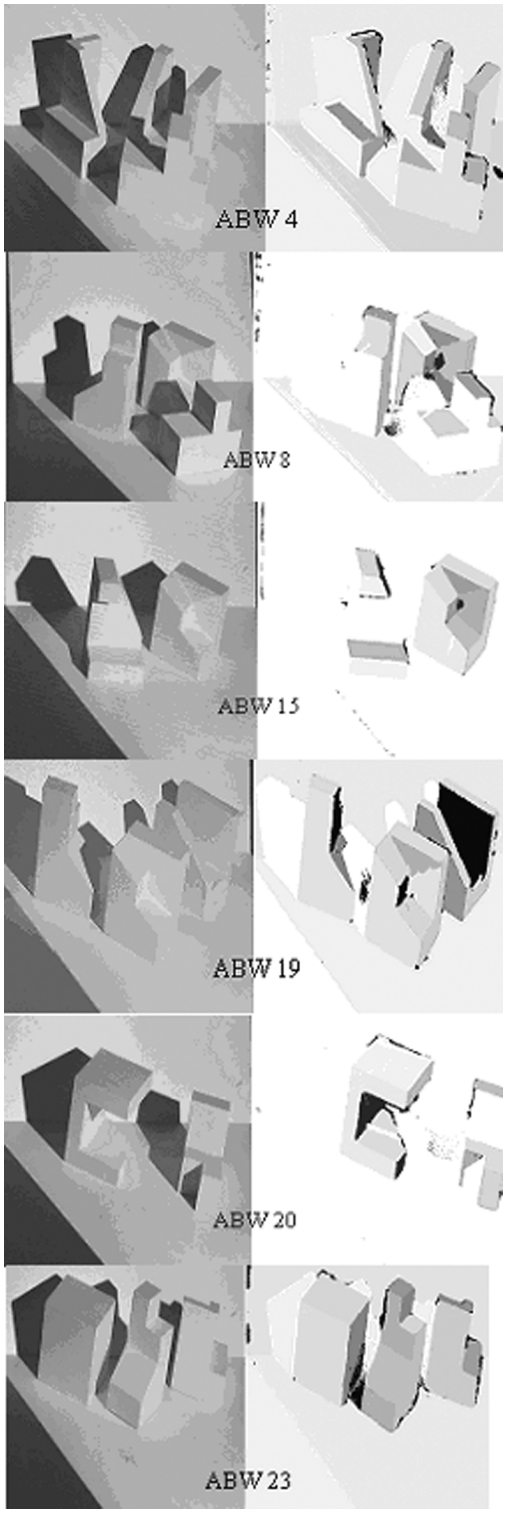

Fig. 3. (Left) Samples of intensity and (right) segmentation result of ABW range image database. The figure shows that the proposed algorithm, although intended for segmenting curved objects, can segment planar objects of the ABW database cleanly and accurately. The complete statistics for the ABW database are given in the above table.

regular grid) required by UB, it is not possible to apply the UB algorithm to the range images shown in Figs. 6–8. However, we have applied UB algorithm to the rest of our database as shown in Figs. 8–14. Consequently, we have not included Figs. 6–8 in the results shown in Table IV. To tune the thresholds for

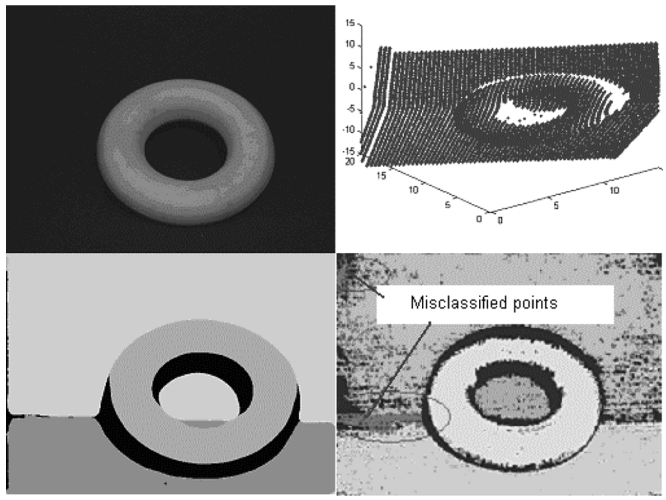

Fig. 4. Sample from the K2T range image database: (top left) intensity image, plotted (top right) range data, (bottom left) segmentation results using the proposed algorithm, and (bottom right) the UB algorithm SSC, as a part of the proposed algorithm, has correctly identified model 3 for the torus part and model 8 for the planar background surfaces.

the UB algorithm, we have changed the parameters of the UB algorithm many times (more than 20) to generate the best performance and the values that generated the best results are shown in Table V.

In our experiments with UB algorithm, we have observed that although the outcome of this algorithm is not much affected by the changes in the value of its threshold named "min region area", it is highly sensitive to the values chosen for the "region acceptance average error" (see [23] for details) thresholds (one for planer and one for curved surfaces). Even changing any of these two thresholds by 10% can significantly change the results.

To incorporate SSC as a model selection criterion in our range segmentation algorithm, we use a surface library (as shown in Table II, which consists of a plane (as the simplest) and a partial-quadratic (as the most general) and six other models with complexities in between. These models are chosen based on the different number of parameters required to express a given data set. For example, because we have cylinders, cones or paraboloids (or parts of them) perpendicular to the xy plane in our objects, then the model $ax^2 + by^2 + cx + dy = 1$ is included in the model library. This model has four parameters whilst the most general model has six parameters. The perpendicular and parallel objects to the xy, xz or yz plane have one or two parameters less than the general model. Therefore, we include them in our library separately (models 2-4). Adding such models to the model library allows our segmentation algorithm to detect such degeneracy (surfaces with axes perpendicular or parallel to range finder coordinate system). It should be noted here that the quadratic models shown in Table II could present different types of conical surfaces based on the signs and values of the parameters.

For all flat surfaces SSC selects model 8 (which represents a flat plane) all the times and also for the curved surfaces the true underlying model is always detected (100% success). For example, surfaces 4 and 2 in Figs. 7 and 8, which are cylinders

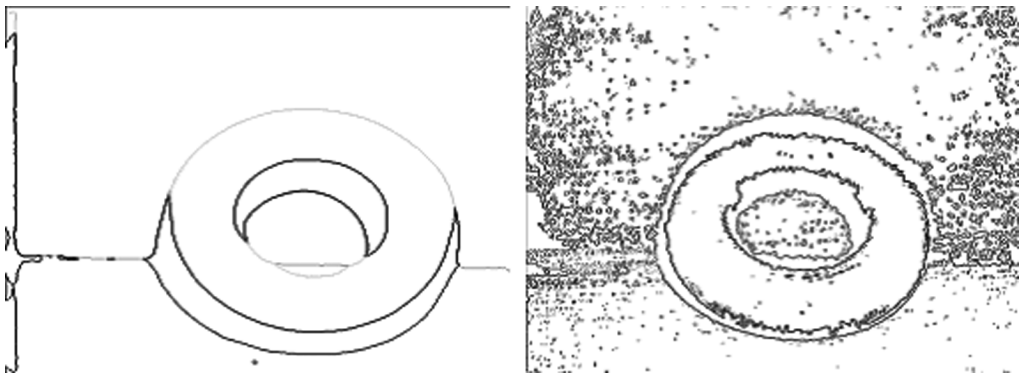

Fig. 5. Edge-detected presentations of the segmentation results shown in Fig. 3—(left) the proposed algorithm and (right) the UB algorithm. The above figures show that the proposed technique produces a cleaner segmentation with sharp edges that are visually in agreement with the available data.

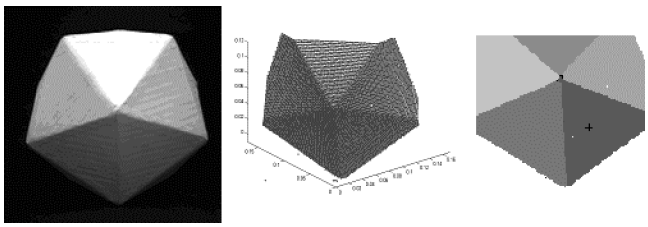

Fig. 6. (Left) Samples of intensity, (middle) plotted range data, and (right) segmentation result of the proposed algorithm. SSC selected Model 8 (plane model) for all of the visible sides of the icosahedron.

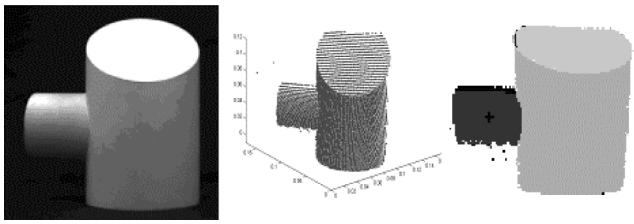

Fig. 7. (Left) Samples of intensity, (middle) plotted range data, and (right) segmentation result of the proposed algorithm. SSC selected model 5 for the cylinder perpendicular to the xy plane (surface 4) and model 3 for the cylinder parallel to the xy plane (surface 5). For surface 6, which is a simple plan, model 8 is chosen by SSC.

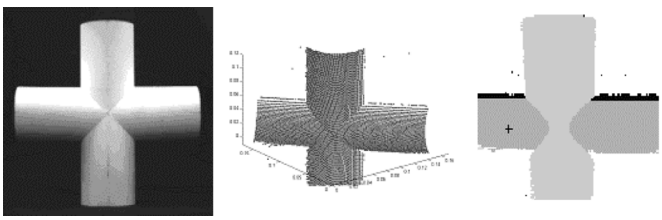

Fig. 8. (Left) Samples of intensity, (middle) plotted range data, and (right) segmentation result of the proposed algorithm. SSC selected model 5 for the cylinder perpendicular to the xy plane (surface 2) and model 3 for the cylinder parallel to the xy plane (surface 3).

perpendicular to the xy plane are identified to have the underlying Model 5. The underlying model for surface 5 and surface 25 in Figs. 7 and 9 was chosen to be Model 3, which is a cylinder parallel to the xy plane. Therefore, our method not only can detect the cylindrical shape of the surface but also it is able to detecting the degeneracy (as explained above) in the data.

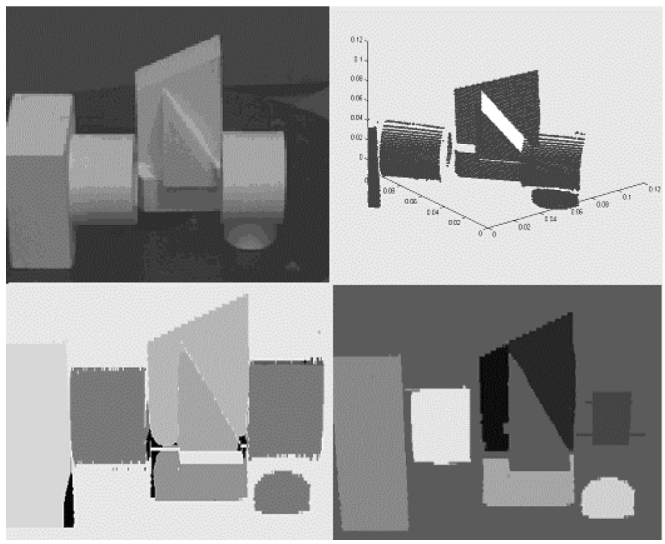

Fig. 9. (Top left) Samples of intensity, (top right) plotted range data, (bottom left) segmentation result of the proposed algorithm, and (bottom right) of UB algorithm. This result illustrates that the proposed algorithm can detect the similarity between two similar cylinders correctly. SSC selected model 3 for the cylinders parallel to the xy plane. The underlying surface models of all planar surfaces are chosen to be model 8 (plane).

One of the important aspects of the proposed algorithm is the way by which it estimates the scale of the noise. Since we obtain the scale of the noise from the data itself, our algorithm is not overly sensitive to the level of noise (and quantisation error) in the range image. Thus, the segmentation algorithm can tolerate a substantial amount of noise. The curved object database that is used in this section consists of many objects made of different materials (metal, wood, cardboard), having different colours and captured in different illumination conditions. As a result, the level of noise is different in the experiments shown here.

One of the advantages of the model-based segmentation over the region-based segmentation algorithms is the way that the model-based algorithms can join the separated objects' parts (for example, segmentation results shown in Figs. 9 and 12–14). As shown in theses figures, the region-growing algorithms (like UB) detect such parts as separate sections while model-based techniques can flag the existing similarities.

The results of our experiments (following figures) show that the proposed technique has been able to correctly segment the

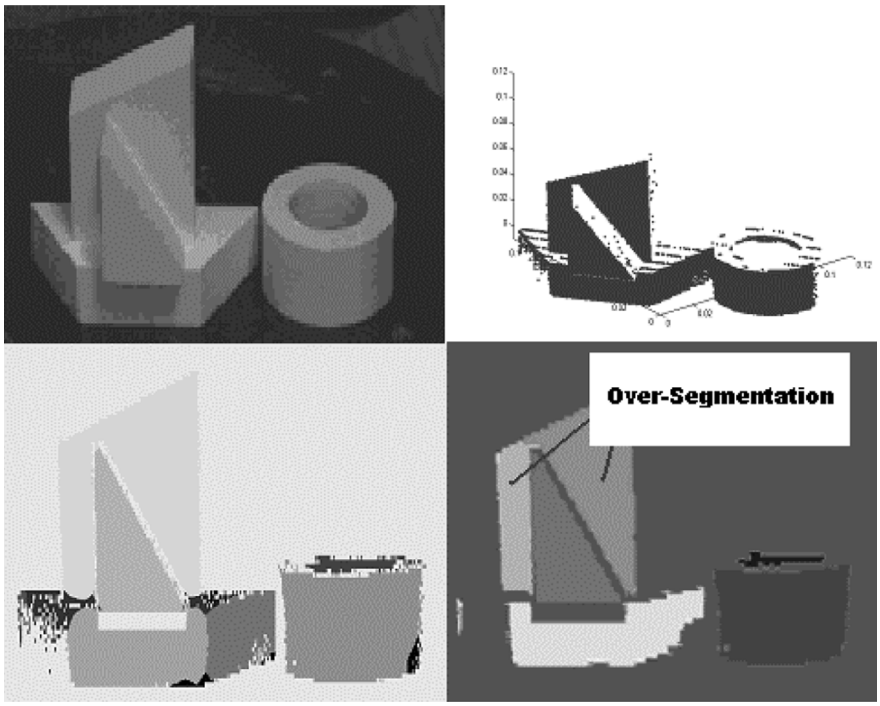

Fig. 10. (Top left) Samples of intensity, (top right) plotted range data, (bottom left) segmentation result of the proposed algorithm, and (bottom right) of UB algorithm. Although the range data contains substantial noise and invalid data, as shown in the plotted range image, the proposed algorithm has accurately segmented the scene. For surface 13, which is a cylinder perpendicular to the xy plane, the model selected is model 5. For all of the planar surfaces, SSC has correctly selected model 8 as the underlying model.

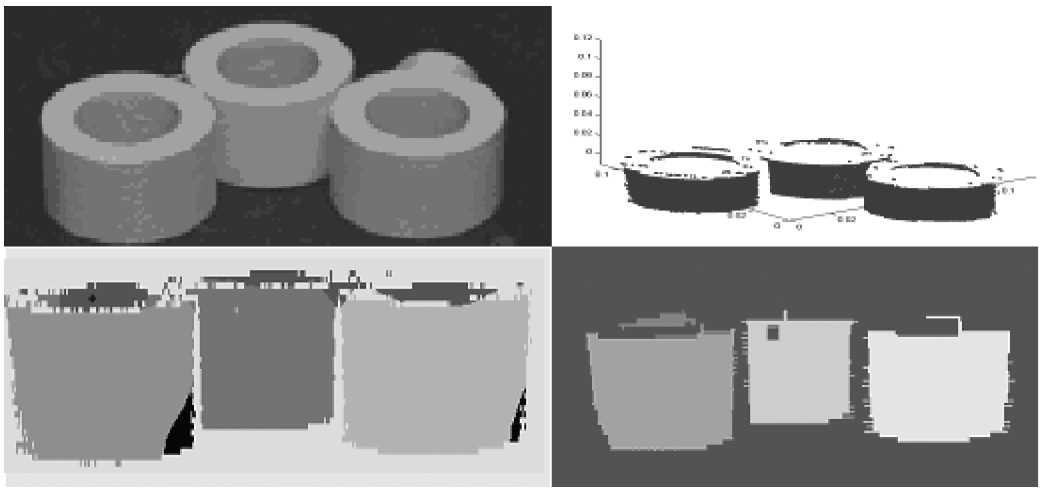

Fig. 11. (Top left) Samples of intensity, (top right) plotted range data, (bottom left) segmentation result of the proposed algorithm, and (bottom right) of UB algorithm. The perpendicular cylinders to the xy plane are detected correctly (model 5) by the SSC.

objects as well as identifying the true type of each surface. In all these figures, the labels show the underlying detected models, which in all cases are in line with our expectations (100% success rate for detecting the underlying model).

In relation to the time complexity of the proposed algorithm, we should note that the time complexity of this method is highly dependent on the number of samples used. In our experiments, which are conducted on a PC with 1.3 Ghz Pentium 4 CPU and 512 MB of RAM running Windows 2000 operating system, the ABW range images (like ABW.10) would take around 65 s to be segmented if we use 500 random samples (times quoted here are from a simple—not optimised—implementation of the algorithm in C and includes time spent on I/O operations). This time reaches 275 s if we use 2500 random samples. The execution time for our own database also takes around 36 to 164 s (on the same machine) depending on the number of samples used. Therefore, a disadvantage of the proposed algorithm in comparison with the UB algorithm is its time complexity.

In our first and second sets of experiments, the objects were made of cardboard or wood (painted white) which are ideal for the rangefinder operation and the results are clean and reliable range images (Figs. 6–12). In the third set of experiments (Figs. 13–15), the objects were made of steel and were sprayed with white powder (to eliminate the specularities of the sur-

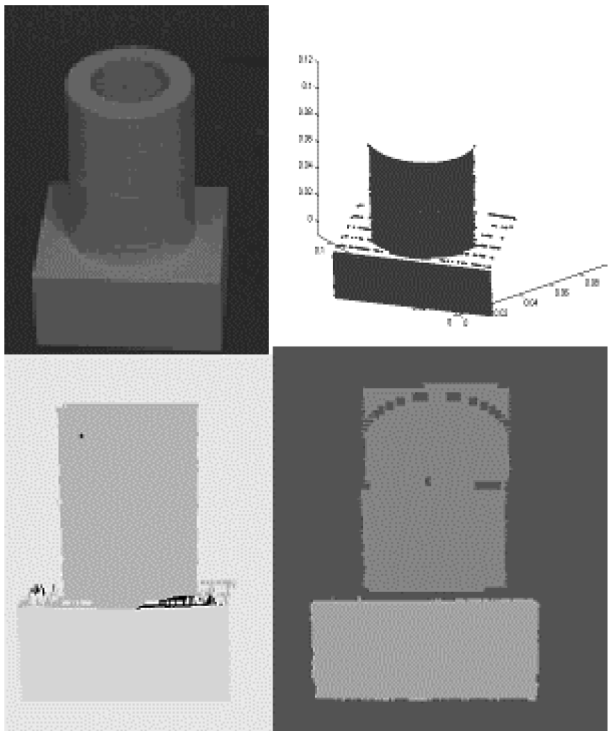

Fig. 12. (Top left) Samples of intensity, (top right) plotted range data, (bottom left) segmentation result of the proposed algorithm, and (bottom right) of UB algorithm. The SSC has selected the correct underlying models for different parts as indicated by the labels.

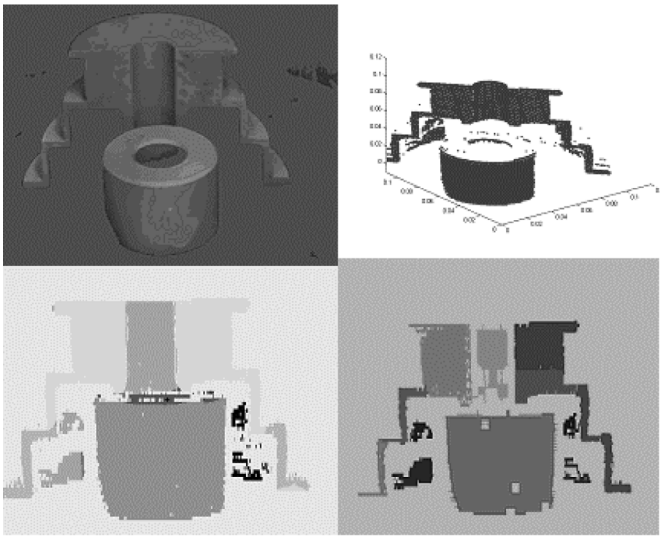

Fig. 13. (Top left) Samples of intensity, (top right) plotted range data, (bottom left) segmentation result of the proposed algorithm, and (bottom right) of UB algorithm. The SSC has selects model 5 for the perpendicular cylinders to the xy plane (surface 16 and surface 15) model 8 for all the planar sections. Surface 17 has two separated planar parts and they are correctly joined together by the proposed technique.

faces). As a result, the range images in this database have a number of missing points and are a bit noisier than the above set (hence, they pose a greater challenge to the segmentation algorithms). The lack of data in some regions is clearly shown in the range data plots of Figs. 13–15.

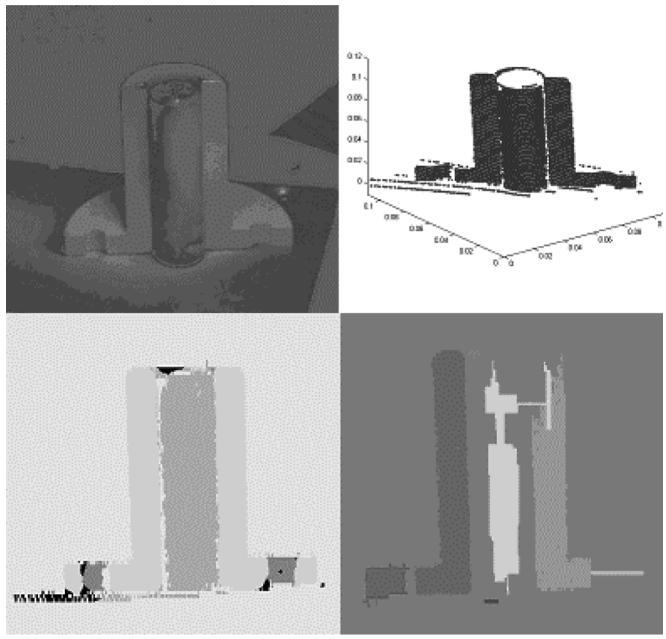

Fig. 14. (Top left) Samples of intensity, (top right) plotted range data, (bottom left) segmentation result of the proposed algorithm, and (bottom right) of UB algorithm. The underlying model for surface 21, which is a cylinder perpendicular to the xy plane, is model 5 and for the flat surface 20 is chosen to be model 8 (plane). Our result correctly indicates that the Surface 20 has two parts separated by Surface 21.

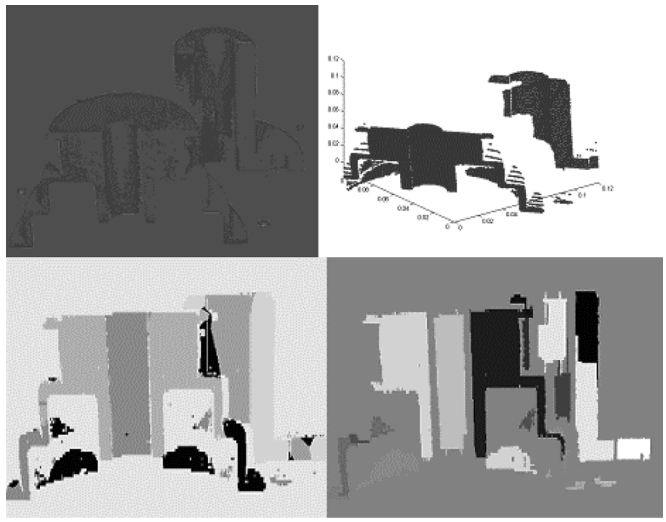

Fig. 15. (Top left) Samples of intensity, (top right) plotted range data, (bottom left) segmentation result of the proposed algorithm, and (bottom right) of UB algorithm. As can be seen from the plotted range data, this range image involves a high number of missed and invalid data. However, SSC can identify the correct underlying model for the cylinder perpendicular to the xy plane (model 5) and also for the flat surfaces (model 8).

TABLE IV
COMPARATIVE RESULTS FOR UB AND THE PROPOSED ALGORITHM ON THE PARAMETRIC RANGE IMAGE DATABASE

Method	Correct Detection	Over Segmentation	Under Segmentation	Missed	Noise
UB[23]	54.5%	27.3%	18.2%	< 0.1%	< 0.1%
Our technique	84.8%	8%	2%	3%	2%

TABLE V
CHOSEN THRESHOLDS FOR EVALUATING THE UB ALGORITHM (SEE [23] FOR DETAILS)

Segment Tolerance	Segment Length	Jump	Crease	Region Area
0.45	3	1	3	50
PRMSE	PAVGERR	CRMSE	CAVGERR	Postprocess Factor
0.005	0.0007	0.011	0.0004	0.2

V. CONCLUSION

In this paper, we have proposed and evaluated a new surface model selection technique called Surface Selection Criterion. Using this criterion, we have been able to develop a robust model-based range segmentation algorithm, which is capable of distinguishing between different types of surfaces while segmenting the objects. The proposed techniques both for model selection and for range segmentation have been extensively tested and have been compared with the state of the art techniques. The proposed criterion for model selection and the resulting segmentation algorithm clearly outperform previously reported techniques.

ACKNOWLEDGMENT

The authors would like to thank Prof. J. Brown for reviewing and proofreading the manuscript; in addition, they would like to thank J. Minack who helped collect the range image database.

REFERENCES

[1] H. Akaike, "A new look at the statistical model identification," *IEEE Trans. Autom. Control*, vol. AC-19, no. 6, pp. 716–723, Dec. 1974.
[2] A. Bab-Hadiashar and D. Suter, "Robust segmentation of visual data using ranked unbiased scale estimate," *ROBOTICA, Int. J. Inf., Education, Res. Robot. Artif. Intell.*, vol. 17, pp. 649–660, 1999.
[3] A. Bab-Hadiashar, N. Gheissari, and D. Suter, "Robust model based motion segmentation," in *Proc. ICPR*, Aug. 2002, pp. 753–757.
[4] A. Bab-Hadiashar and N. Gheissari, "Model selection for range segmentation of curved objects," in *Proc. 8th Eur. Conf. Computer Vision*, 2004, pp. 83–94.
[5] P. J. Besl and R. C. Jain, "Segmentation through variable-order surface fitting," *IEEE Trans. Pattern Anal. Mach. Intell.*, vol. 10, no. 3, pp. 167–192, Mar. 1988.
[6] M. E. Bock and C. Guerra, "A geometric approach to the segmentation of range images," in *Proc. 2nd Inf. Conf. 3-D Imaging and Modeling*, Oct. 1999, pp. 261–269.
[7] ——, "Segmentation of range images through the integration of different strategies," presented at the 6th Int. Workshop Vision Modeling and Visualization, Stuttgart, Germany, 2001.
[8] K. L. Boyer, M. J. Mirza, and G. Ganguly, "The robust sequential estimator: A general approach and its application to surface organization in range data," *IEEE Trans. Pattern Anal. Mach. Intell.*, vol. 16, pp. 987–1001, Oct. 1994.
[9] H. Bozdogan, "Model selection and akaike's information criterion (AIC): The general theory and its analytical extensions," *Psychometrica*, vol. 52, pp. 345–370, 1987.
[10] K. Bubna and V. C. Stewart, "Model selection and surface merging in recognition algorithms," in *Proc. ICCV*, Bombay, India, 1998, pp. 895–902.
[11] D. Chickering and D. Heckerman, "Efficient approximation for the marginal likelihood of bayesian networks with hidden variables," *Mach. Learn.*, vol. 29, no. 2–3, pp. 181–212, 1997.
[12] T. J. Fan, G. Medioni, and R. Nevatia, "Segmented descriptions of 3-D surfaces," *IEEE Trans. Robot. Autom.*, vol. 3, no. 6, pp. 527–538, Dec. 1987.
[13] T. U. Fan, G. Medioni, and R. Nevatia, "Rocognising 3-D objects using surface descriptions," *IEEE Trans. Pattern Recognit. Mach. Intell.*, vol. 11, no. 11, pp. 1140–1157, Nov. 1989.
[14] O. D. Faugeras and M. Hebert, "Segmentation of range data into planar and quadratic patches," in *Proc. IEEE Conf. Computer Vision and Pattern Recognition*, Arlington, VA, Jun. 1983, pp. 8–13.
[15] A. W. Fitzgibbon, D. W. Eggert, and R. B. Fisher, "High-level cad model acquisition from range images," *Comput.-Aided Design*, vol. 29, pp. 321–330, 1997.
[16] N. Gheissari and A. Bab-Hadiashar, "Model selection criteria in computer vision: Are they different," in *Proc. Digital Image Computing Techniques and Applications*, Dec. 2003, pp. 185–194.
[17] D. B. Goldgof, T. S. Huang, and H. Lee, "A curvature-based approach to terrain recognition," *IEEE Trans. Pattern Anal. Mach. Intell.*, vol. 11, no. 11, pp. 1213–1217, Nov. 1989.
[18] H. Gu, Y. Shirai, and M. Asada, "MDL-based segmentation and motion modeling in a long sequence of scene with multiple independently moving objects," *J. Pattern Recognit. Soc.*, vol. 28, pp. 781–793, 1995.
[19] R. L. Hoffman and A. K. Jain, "Segmentation and classification of range images," *IEEE Trans. Pattern Anal. Mach. Intell.*, vol. 9, no. 5, pp. 608–620, Sep. 1987.
[20] A. Hoover, USF Range Image Database.
[21] A. Hoover, G. Jean-Baptist, X. Jiang, J. P. Flynn, B. Horst, D. Goldgof, K. Bowyer, D. Fggert, A. Fitzgibbon, and R. Fisher, "An experimental comparison of range image segmentation algorithms," *IEEE Trans. Pattern Anal. Mach. Intell.*, vol. 18, no. 7, pp. 673–689, Jul. 1996.
[22] X. Jiang, K. Bowyer, Y. Morioka, S. Hiura, K. Sato, S. Inokuchi, M. Bock, C. Guerra, R. E. Loke, and J. M. H. d. Buf, "Some further results of experimental comparison of range image segmentation," in *Proc. Int. Conf. Pattern Recognition*, Barcelona, Spain, Sep. 2000, pp. 877–881.
[23] X. Jiang and H. Bunke, "Range image segmentation: Adaptive grouping of edges into region," in *Proc. Asian Conf. Computer Vision*, Hong Kong, 1998, pp. 299–306.
[24] X. B. H. Jiang, "Edge detection in range images based on scan line approximation," *Comput. Vis. Image Understand.*, vol. 73, pp. 183–199, Feb. 1999.
[25] K. Kanatani, "Model selection for geometric inference," in *Proc. ACCV*, Melbourne, Australia, pp. xxi–xxxii.
[26] ——, "Evaluation and selection of models for motion segmentation," in *Proc. 7th Eur. Conf. Computer Vision*, Dec. 2002, pp. 335–349.
[27] ——, "Model selection for geometric inference," in *Proc. 5th Asian Conf. Computer Vision*, Melbourne, Australia, Jan. 2002, pp. xxi–xxxii.
[28] ——, "Model selection criteria for geometric inference," in *Data Segmentation and Model Selection for Computer Vision: A Statistical Approach*, A. Bab-Hadiashar and D. Suter, Eds. New York: Springer-Verlag, 2000, pp. 91–118.
[29] K. Koster and M. Spann, "MIR: An approach to robust clustering-application to range image segmentation," *IEEE Trans. Pattern Anal. Mach. Intell.*, vol. 22, no. 5, pp. 430–444, May 2000.
[30] R. E. Loke and J. M. H. d. Buf, UALG-ISACS-TR03, Univ. Algarve, Mar. 1998.
[31] C. L. Mallows, "Some comments on CP," in *Technometrics*, 1973, vol. 15, pp. 661–675.
[32] D. Marshall, G. Lukacs, and R. Martin, "Robust segmentation of primitives from range data in the presence of geometric degeneracy," *UALG-ISACS-TR03*, vol. 23, no. 3, pp. 304–314, Mar. 2001.
[33] G. Medioni and B. Parvin, "Segmentation of range images into planar surfaces by split and merg," in *Proc. IEEE Conf. Computer Vision and Pattern Recongnition*, 1986, pp. 415–417.
[34] M. W. Powell, K. Bower, X. Jiang, and H. Bunke, "Comparing curved-surface range image segmentors," in *Proc. 6th Int. Conf. Computer Vision*, Bombay, India, 1998, pp. 286–291.
[35] J. Rissanen, "Universal coding, information, prediction and estimation," *IEEE Trans. Inf. Theory*, vol. IT-30, no. 4, pp. 629–636, Jul. 1984.
[36] ——, "Modeling by shortest data description," *Automatica*, vol. 14, pp. 465–471, 1978.
[37] E. Ronchetti, C. Field, and W. Blanchard, "Robust linear model selection by cross-validation," *J. Amer. Statist. Assoc.*, vol. 92, pp. 1017–1023, 1997.
[38] P. J. Rousseeuw and A. M. Leroy, *Robust Regression and Outlier Detection*. New York: Wiley, 1987.
[39] G. Schwarz, "Estimating the dimension of a model," *Ann. Statist.*, vol. 6, pp. 461–464, 1978.
[40] P. S. Timoshenko and S. W. Krieger, "Theory of plates and shells," in *Pure Bending of Plates*, P. S. Timoshenko and S. W. Krieger, Eds. New York: McGraw-Hill, 1959, ch. 2, pp. 46–47.

[41] P. Tissainayagam and D. Suter, "Visual feature tracking with automatic motion model selection," in *Proc. JCIS*, Nov. 1998, pp. 322–325.
[42] P. H. S. Torr, "An assessment of information criteria for motion model selection," in *Proc. IEEE Conf. Computer Vision and Pattern Recognition*, 1997, pp. 47–53.
[43] ——, "Geometric motion segmentation and model selection phil," *Trans. Roy. Soc. Lond.*, vol. 356, pp. 1321–1340, 1998.
[44] ——, "Model Selection for Two View Geometry: A Review," in *Shape, Contouring and Grouping in Computer Vision*. London, U.K.: Springer-Verlag, 1999, pp. 277–301.
[45] ——, "Model selection for structure and motion recovery from multiple images," in *Data Segmentation and Model Selection for Computer Vision: A Statistical Approach*, A Bab-Hadiashar and D Suter, Eds. New York: Springer-Verlag, 2000, pp. 143–181.
[46] ——, "Bayesian model estimation and selection for epipolar geometry and generic manifold fitting," *Int. J. Comput. Vis.*, vol. 50, pp. 35–61, 2002.
[47] E. Trucco and R. B. Fisher, "Experiments in curvature-based segmentation of range data," *IEEE Trans. Pattern Anal. Mach. Intell.*, vol. 17, no. 2, pp. 3177–182, Feb. 1995.
[48] V. J. L. Vliet and W. P. Verbeek, "Curvature and bending energy in digitized 2D and 3D images," in *Proc. 8th Scandinavian Conf. Image Analysis*, Tromso, Norway, 1993, pp. 1403–1410.
[49] N. Werghi, R. B. Fisher, C. Robertson, and A. Ashbrook, "Modeling objects having quadratic surfaces incorporating geometric constraints," in *Proc. 5th Eur. Conf. Computer Vision*, 1998, pp. 185–201.

Alireza Bab-Hadiashar (SM'04) was born in Iran in 1964. He received the Bachelor of Engineering, Master of Engineering, and Ph.D. degrees in 1988 from the University of Tehran, Tehran, Iran, in 1994 from the University of Sydney, Sydney, Australia, and in 1997 from Monash University, Australia, respectively.

Since 1997, he has held various academic positions at both Monash University and the Swinburne University of Technology, Melbourne, Australia, where he is currently an Associate Professor and Program Coordinator of Robotics and Mechatronics Engineering. His research interest is the development robust data analysis techniques for engineering applications, in general, and computer vision, in particular.

Niloofar Gheissari was born in Iran in 1977. She received the Engineering honours degree in Software Engineering from the Isfahan University of Technology, Iran, in 2000, and the Ph.D. degree from the Swinburne University of Technology, Melbourne, Australia, in 2004. Her Ph.D. thesis concerned model-based segmentation of visual data.

Since 2005, she has worked in different research areas for National ICT Australia, Australian National University, Canberra, where she is currently a Postdoctorate Researcher. Her research interest is in different areas of computer vision, including segmentation, motion estimation, tracking, and object recognition.